

The Electrical Properties of Cementitious Sealants for Subsea CCS Applications

G. Starrs, B. Suryanto

Institute for Sustainable Built Environment, Heriot-Watt University, Edinburgh, United Kingdom

ABSTRACT

A range of cementitious sealants designed for use in the storage of carbon dioxide within repurposed sub-sea oilwells were studied using electrical properties measurements. Electrical Resistance measurements were used to track the hydration profiles of the sealants during an enhanced curing regime at high pressure and temperature. The post curing properties of the sealants were further examined using multi-frequency Impedance measurements at room temperature and atmospheric pressure. Results for both stages are presented.

Keywords: CCS, cementitious sealants, curing, resistance, impedance spectroscopy.

1.0 INTRODUCTION

1.1 Cementitious Sealants for CCS

Cementitious sealant materials are an important component of systems intended for the sealing of discontinued North Sea oilwells that have been repurposed for the storage of CO₂ captured as part of CCS (Carbon Capture and Storage) operations. **Figure 1** (Gasda et al, 2004) represents the structure of a plugged wellbore with the potential leakage paths of liquid or dissolved carbon dioxide highlighted. These can include a) the external casing/sealant interface, b) the internal casing/sealant interface, c) the sealant body microstructure, d) fractured casing, e) fractured sealant, and f) the external sealant/rock interface.

It is the purpose of the CEMENTTEGRITY project funded through ACT3 (Accelerating CCS Technologies project No 327311 – see www.cementegrity.eu) to investigate the performance characteristics of wellbore sealants that could ensure long term sealing effectiveness during CO₂ storage (e.g. Van Noort et al, 2023). As part of CEMENTTEGRITY, research is being conducted at Heriot Watt University into the **electrical properties** of a range of sealant materials, both during and after an enhanced curing regime that synthesizes aspects of the in-situ environmental conditions of a subsea wellbore.

1.2 Electrical Properties Measurements

There is known to be a correlation between the electrical properties of cementitious materials and their mechanical performance (McCarter and Starrs, 2002). This correlation is mediated via their microstructural characteristics – determined by pore structure and the presence of water therein (at gauging and during later development).

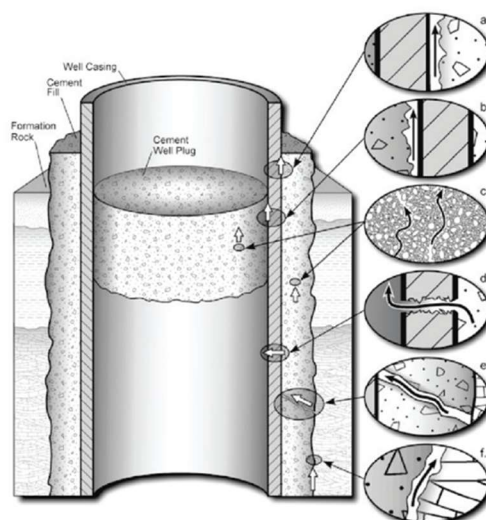


Fig.1. Schematic representation of a plugged well, showing potential leakage pathways.

Thus, electrical properties measurements may be useful in characterising and monitoring well-plug sealant performance and possibly aspects of sealant/casing integrity. Such properties can be analysed by means of **Impedance Spectroscopy**, whereby a material system's current response to a frequency-variable alternating voltage stimulus, mediated through a suitable electrode interface, can provide insight into aspects of the system's underlying microstructure. **Impedance**, $Z(\omega)$, where ω is angular frequency, is a complex number and is the ratio of applied voltage, $V(\omega)$, to resultant current, $I(\omega)$. It obeys Ohm's Law as shown by **Equation 1**.

$$Z(\omega) = Z'(\omega) - jZ''(\omega) = \frac{V(\omega)}{I(\omega)} \text{ Ohm} \quad (1)$$

Where j is the complex operator. Real Impedance, Z' , is Resistance, and Imaginary Impedance, Z'' , is Reactance. As $\omega \rightarrow 0$, Impedance becomes a pure Resistance.

As the Impedance of cementitious materials is frequency variable, such variations can provide insight into the

underlying structure, and hence performance. This abstract presents and discusses laboratory experimental examples of such properties measurements.

2.0 EXPERIMENTAL PROGRAMME

2.1 Materials and Sample Preparation

The sealant materials studied in this work are presented in **Table 1**. Sealant S1 is a standard G-class OPC (British Standards Institution, 2000) with 35% replacement by silica flour and is included as a baseline reference for comparison. The other sealants are proprietary materials whose details are not fully disclosed.

Table 1. Sealants examined in current study.

Sealant	Material Content	Description
S1	OPC with 35% silica	Old oilwell reference
S2	Modified S1 plus minerals addition	Currently used for low-permeability
S3	Modified S1 plus Restone mineral	Modified blend - CO ₂ sequestering
S4	Calcium Aluminate cement system	Acid resistant - used at high temperature
S5	Granite based Geopolymer	1-part system designed for CCS

Sealants S2 and S3 are OPC based. However, S2 has an unspecified amount of mineral additions, designed to produce very low permeability – a desired sealant trait. S3 is a blend containing RePlug®, a mineral addition (see <https://restone.no/replug/>) conferring a CO₂ sequestering facility. S4 is a proprietary calcium aluminate system currently deployed in high temperature wells and considered highly acid resistant. S5 is a geopolymer sealant engineered specifically for CCS.

Experimental samples take the form of small steel cylinders (50.8mm OD, 44mm ID, 50mm length) into which is moulded a sealant prism with 40mm diameter ends protruding 10mm. The moulded shape is facilitated by two PTFE end caps which encapsulate the material during curing. Such samples are miniature versions of the sealant-plug/casing well-head represented in **Figure 1**.

As shown in **Figure 2** there are two electrode configurations. In the 2-pin parallel-pair type, two marine grade steel rods of 2.4 mm diameter, separated by 15 mm are inserted through the full length of the sample. In the 1-pin Coaxial type, a single 2.4 mm diameter rod runs through the centre of the sample. The Coaxial type facilitates impedance measurements via the steel casing, thereby including the sealant/casing interface.

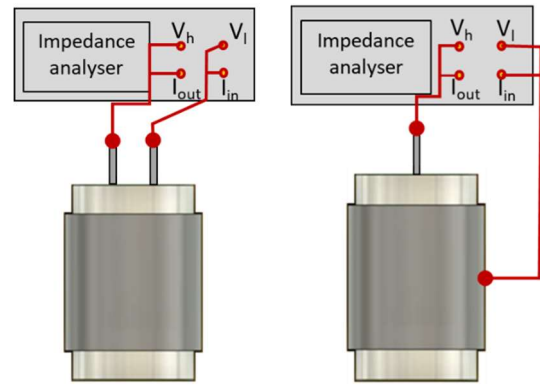


Fig.2. 2-Pin (left) and Coaxial (right) Electrode Systems.

2.2 Sealant Curing Regime

All samples were prepared and cured at the Haliburton facility in Stavanger, Norway, where autoclave equipment capable of the required enhanced curing regime is located (see **Figure 3**).



Fig. 3. Autoclave/logging system during curing process.

Once the material is gauged and sealed in the moulds, these are then placed in the autoclave chamber(s). For each sealant, two samples of the 2-pin electrode type are connected to a logging system capable of tracking *in-situ* low frequency (i.e. direct current) Resistance during the curing period. However, these samples are housed in a chamber where the containment fluid is non-conducting oil rather than water so as not to contaminate the electrical measurements. Other samples are placed in a separate chamber with water as the containment fluid.

The 2-pin electrode samples, ready for containment in the autoclave system, are shown in **Figure 4**.

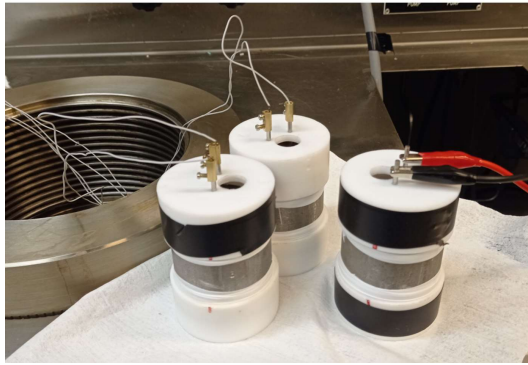


Fig. 4. 2-pin electrode sample prior to curing regime

The curing regime is summarised graphically in **Figure 5**. The autoclave system is pressurised to 300 bars, then the internal temperature is raised over a period of 4 hours to 80°C where it is held for 3 days. The temperature is then raised from 80°C to 150°C over 7 days and held at 150°C for 21 days. From 31.33 days the temperature is lowered steadily from 150°C to 20°C over a period of 7 days. When 100°C is reached during this phase the internal pressure is released and the chamber(s) allowed to reach equilibrium. The samples are removed from the autoclave after 38.33 days once they have stabilised at 20°C.

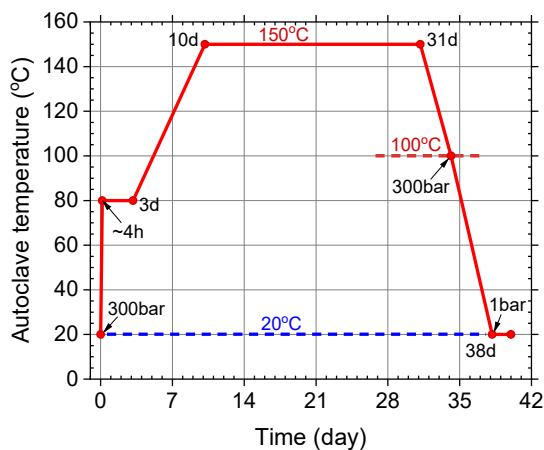


Fig. 5. Graphical summary of curing regime.

3.0 RESULTS AND DISCUSSION

3.1 Resistance Measurements S1 – S5

During the curing regime, **Resistance** data is gathered every 10 minutes, tracking the sealant hydration and hardening process. This is achieved using a bespoke logging system developed for Heriot-Watt (Chrisp et al, 2010) for measurements on OPC based mortar and concrete.

The Resistance profiles of sealants S1 to S5 during curing are presented with the temperature profile in **Figure 6**. For hydraulic cements the general response would be for Resistance to fall as temperature is increased. The Resistance is observed to be correlated to temperature throughout curing but with each sealant showing measurably different absolute values of resistance as well as individual distinguishing characteristics as hydration proceeds.

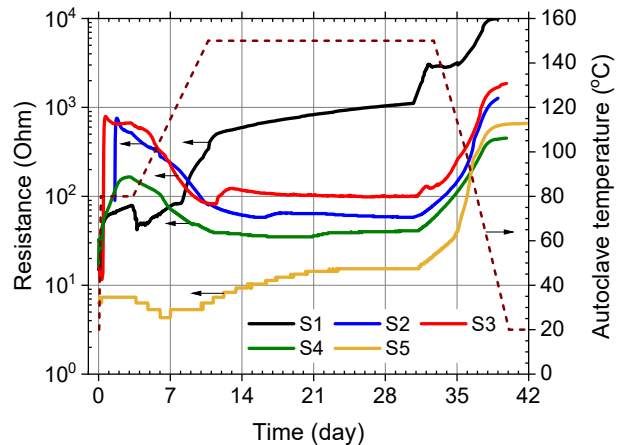


Fig. 6. Resistance profile of sealants during curing.

For example, for S1 during the initial 3 days at 80°C a gradual increase in resistance is observed reflecting early development of a pore structure due to OPC hydration. The trend is then reversed briefly once temperature starts to increase, as would be expected, with Resistance dropping. As temperature continues to increase the accelerating hydration and pore development overcome this tendency and Resistance resumes rising. The steepness of the rise increases at ~150°C, indicating the engagement of silica flour in the hydration process. Once the temperature is stable at 150°C the Resistance continues to rise much less steeply and then levels off at ~28 days indicating that the material is almost fully cured.

Similar patterns are observed for the other sealants but with modifications at key stages due to the individual additions present. For example, S2 and S3 have similar curing profiles but S3 has a sudden rise in Resistance on reaching 150°C that quickly levels off, possibly indicating engagement of the ReStone mineral component in the hydration process. S5, the 1-part geopolymer, has the simplest response of the sealants. It shows no immediate evidence of hydration until temperature reaches ~115°C at which point the Resistance begins to increase. The increase continues until 22 days then levels off as curing is largely complete.

All sealants show a similar general steep rise in Resistance as the temperature falls from 150°C to 20°C at the end of curing, but the individual rate, and profile, for each suggests distinguishable thermal activation characteristics.

3.1 Impedance Measurements S1 – S4

In the post-curing period, Impedance spectra for sealants S1 to S4 were gathered by means of a Solartron 1260 Impedance Analyser from the 1-pin Coaxial samples cured in water. The results are presented in **Figure 7** in Nyquist diagram format, with Reactance plotted as a function of Resistance as frequency increases from 1Hz to 10MHz.

The plots for S1, S2 and S3 show a visually similar pattern proceeding from right to left as frequency is increased. This is essentially a long tail and a shallow arc conjoined at a cusp point where the Reactance reaches a minimum value. Superficially, this is the same pattern shown by plain OPC (McCarter, 1994). The right-hand tail (low

frequency section) of the response is determined not simply by the sample material properties but largely by the interaction of the material and electrodes at their interface. In this case this includes the sealant/casing interface. It is observable that the absolute impedance values as well as the frequency characteristics of this part of the response are distinguishable for each sealant.

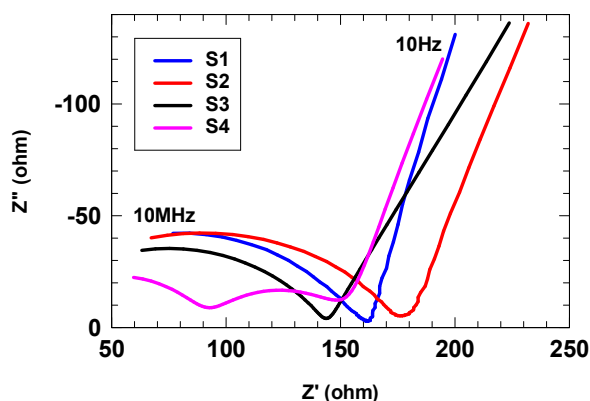


Fig. 7. Post-curing Impedance plots of sealants S1-S4

Of interest is the response of sealant S4, in that it reveals a *dual-arc* feature. It is notable that this sealant is derived from a different cementitious material (calcium aluminate) and contains several undisclosed proprietary additions. Similar features have previously been observed in OPC based materials containing supplementary additions (Starrs and McCarter, 1998).

Table 2 presents significant frequencies discernible on the Impedance response of each sealant. These are:

- The point at which Reactance is at a minimum (the cusp point dividing the bulk material response from the material/electrode interface response).
- The point at which the bulk arc Reactance is at a maximum.

Table 2. Significant Frequency Points in Impedance Plots.

Sealant	Cusp Point	Bulk Arc Maximum
S1	2.5 kHz	8.0 MHz
S2	6.3 kHz	5.0 MHz
S3	10 kHz	6.3 MHz
S4	400 Hz, 250 kHz	5.0 kHz

The Resistance at the cusp frequency is usually taken as indicative of the true bulk value at zero frequency. Note, however, that because the dual cusp effect in the S4 response occurs at very low and very high frequencies, it is likely that true bulk Resistance lies somewhere on the middle arc, complicating interpretation.

4.0 CONCLUSIONS

Five cementitious sealant materials, designed for use in repurposed oilwell CCS systems, have been subject to electrical properties measurements.

The sealants were encapsulated in steel tubes to produce cylindrical samples designed to mimic a plugged wellbore

in miniature. Two two-electrode configurations were used to allow Impedance measurements on the sealants. An embedded parallel-pair electrode system was used to gather in-situ Resistance measurements during a 39-day enhanced curing regime at high temperature and pressure (150°C, 300bars). A coaxial system, using an embedded central electrode, with the steel casing as the outer electrode, was used in the post-curing period to obtain multi-frequency Impedance data at 20°C and atmospheric pressure.

The in-situ Resistance of S1 to S5 reveals distinctive features of the hydration process for each sealant, as well as different individual thermal activation characteristics during the post-curing controlled-cooling phase.

The post-curing Impedance measurements for S1 to S4 reveal distinguishing characteristics for each sealant at the bulk material level (particularly for S4), as well as discernible differences in the low frequency response of the sealant/steel-casing interface.

ACKNOWLEDGEMENTS

The authors wish to express gratitude for funding from the UK Government Department for Energy Security & Net Zero (through the UK ACT ERA - NET EC GRANT AGREEMENT 691712).

The authors are also grateful to Haliburton for the provision of experimental facilities at the EESSA Technology laboratory located in Tananger, Stavanger, in Norway, and for the personal assistance of Espen Sorensen in the running of experiments.

REFERENCES

- British Standards Institution, EN197-1:2000, Cement-Part 1: Composition, Specifications and Conformity Criteria for Common Cements. BSI: London, 2000.
- Chrip, T.M., Starrs, G., McCarter, W.J., 2010. Developments in Intelligent Monitoring of Concrete Structures, Proceedings of the 13th International Conference on Structural Faults and Repair, Edinburgh.
- Gasda, S.E., Bachu, S., Celia, M.A., 2004. The Potential for CO₂ Leakage from Storage Sites in Geological Media: Analysis of Well Distribution in Mature Sedimentary Basins, *Environmental Geology*, 46(6-7), 707-720.
- McCarter W.J., Starrs G., Chrip T.M., 2002. Electrical monitoring methods in cement science. In: P. Barnes and J. Bensted (Eds.), *Structure and Performance of Cements*, Second Edition, Spon Press, London, 442–456 (ISBN 0-203-47778-2).
- McCarter, W. J., 1994, A parametric study on the impedance characteristics of cement-aggregate systems during early hydration, *Cem. Conc. Res.*, 1994, 24 (6), 1097-1110.
- Starrs G., McCarter W.J., *Immittance of Cementitious Binders during early Hydration*. *Advances in Cement Research*, 1998, 10(4), 179-186.
- Van Noort, Suryanto, B., Starrs, G., Lende, G., 2023 Testing and developing improved wellbore sealants for CCS applications. 12th Trondheim Carbon Capture and Storage Conference (TCCS), 19/06-21/06, Trondheim (N).